Proceedings of the ASME 2010 3rd Joint US-European Fluids Engineering Summer Meeting and
8th International Conference on Nanochannels, Microchannels, and Minichannels
FEDSM-ICNMM2010
August 1-5, 2010, Montreal, Canada

FEDSM-ICNMM2010-30792

EXPERIMENTAL STUDY ON SINGLE PHASE FLOW IN MICROCHANNELS AT HIGH MASS FLOW RATES

Mehmed Rafet Özdemir
Sabancı University MSc. Student
İstanbul, Turkey

Ali Koşar
Sabancı University Faculty Member
İstanbul, Turkey

ABSTRACT

With the increasing speed and decreasing size of current microprocessors and microchips the dimensions of their heat sinks are continuously shrinking from mini size to micro size. The most extensively used and practical micro heat sinks are plain microchannels which find applications in many areas besides electronics cooling such as in microreactors, fuel cells, drug delivery, micropropulsion and automotive industry. Because of their widespread usage, they attracted the attention of many researchers, which gave rise to many studies on single-phase as well as on flow boiling.

The proposed study aims at filling the gap in heat and fluid flow in microchannels at high mass velocities in the literature. For this purpose single-phase fluid (de-ionized water) flow was investigated over a broad range of mass velocity (1300 kg/m^{2}s-7200 kg/m^{2}s) in a microtube with an inner diameter of ~ 250 μm. Besides comparing the experimental results in fully developed flow to the theory, the focus of this study is on thermally developing flows. Wall temperatures and pressure drops were measured and processed to obtain heat transfer coefficients, Nusselt numbers and friction factors. It was found that the existing theory about developing flows could fairly predict experimental data on developing flows in microscale for both laminar and turbulent conditions.

INTRODUCTION

In the last decade mini/micro scale devices have found many application areas such as aerospace, mechanical, biological, chemical and optical applications. Single phase heat transfer has been considered as an important heat removal mechanism for cooling applications in micro scale and was proposed as a prominent thermal management solution. Many experimental studies on microchannels related to the laminar flow [1-3], laminar to turbulent transition [4-11,19-21] and turbulent flow [12-15] are present in literature. These studies indicate that the existing theory could provide reasonable predictions under laminar and turbulent flow conditions, while the agreement between the theory and experiemntal results was not very good in laminar-turbulent flow transition.

There are few experimental studies present in the literature related to thermally developing flows on single phase flow in microchannels [11,16,17] because typically high pressures are needed for having thermally developing flows, where high flow rates should be attained to see significant developing effects along microchannels. With the change in bulk fluid temperature at high flow rates, the flow may also become turbulent at a certain location downstream the inlet of the channel as a consequence of fluid property changes. Particularly for short microchannels, developing effects could be sensed at high flow rates and the resulting increased heat transfer characteristics could be greatly exploited in many applications. The present study is aimed to fill the lack of information about single phase flow under these conditions in micro scale. Moreover, with the enhancement in micropumping capabilities, single phase flow could be performed at higher mass velocities so that the gap in this area could be filled with new studies. New emerging technologies resulting in local heating such as nano-scale plasmonic applications [22-24] and near field radiative energy exchange between objects [25-28] could greatly benefit from single phase heat transfer at high flow rates in micro/nano-scale.

To investigate single phase flow at high flow rates in micro scale, an experimental study was conducted at high flow rates in micro tubes with a inner diameter of 250 micrometers. De-ionized water was used as working fluid, and the test section was heated by Joule heating. Mass flux was changed from 1300 kg/m^2s to 7200 kg/m^2s, and heat transfer coefficients were deduced from local temperature measurements.

NOMENCLATURE

A_c	Cross sectional area m^2.
A_s	Heated area m^2.
c_p	Specific heat at constant pressure J kg^{-1} $^oC^{-1}$.
d_i	Inner channel diameter m.
D_h	Hydraulic diameter m.
f	Friction factor.
G	Mass velocity kg m^{-2} s^{-1}.
h_{sp}	Single phase heat transfer coefficient W m^{-2} $^oC^{-1}$.
k_w	Thermal conductivity of the wall W m^{-1} $^oC^{-1}$.
k_f	Thermal conductivity of the fluid W m^{-1} $^oC^{-1}$.
L	Channel length m.
L_h	Heated length m.
$\dot{m}$	Mass flow rate kg s^{-1}.
MAE	Mean Absolute Error.
Nu	Nusselt number.
$Nu_{x,H1}$	Thermally developing nusselt number depending x.
$Nu_{m,H1}$	Mean thermally developing nusselt number.
Nu_{∞}	Fully developed Nu_H.
P	Electrical power W.
P_r	Prandtl number.
$\dot{q}$	Volumetric heat generation W m^{-3}.
q”	Heat flux W/cm^2.
$\dot{Q}_{loss}$	Heat loss W.
Re	Reynolds number.
r_o	Outer channel radius m.
r_i	Inner channel radius m.
T_e	Exit temperature ºC.
T_i	Inlet fluid temperature ºC.
T_f	Fluid temperature ºC.
$T_{w,i}$	Local inner surface temperature of the microchannel ºC.
$T_{w,o}$	Local outer surface temperature of the microchannel ºC.
x	Developing length m.
x_{th}	Thermocouple location m.
z	Microchannel inner surface length m.

Greek:

ΔP	Pressure Drop kPa.
ρ_f	Fluid Density kg m^{-3}.
μ	Viscosity kg m^{-1} s^{-1}.

EXPERIMENTAL TEST SETUP AND PROCEDURE

Experimental Test Setup

The experimental setup consists of the test section, a storage cylinder, an Omega® flow meters, pressure sensors and proper tubing and fittings. Two alligator clips, each 3 mm wide, were attached to the heated length on the microtube surface. They were installed with a prescribed distance (heated length) from each other and were connected to a high current power supply with an adjustable DC current and high power output to provide Joule heating to the 14.88 cm long micro tube of ~ 254µm inner diameter. The heated length was adjusted to 5.65cm.

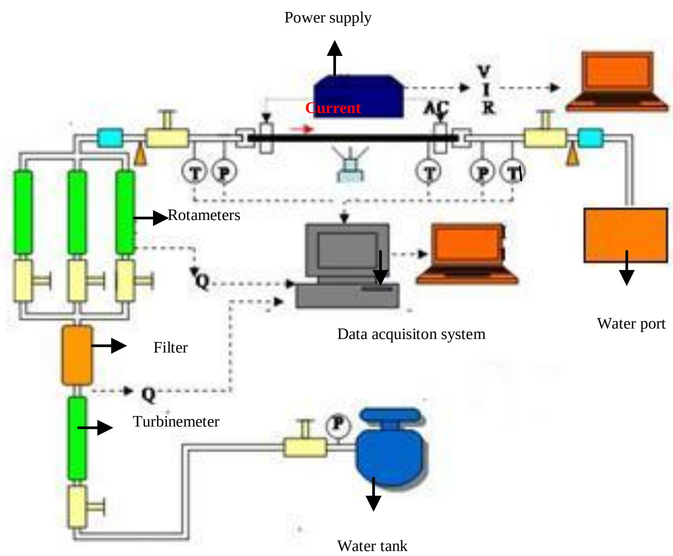

Figure 1 Experimental Setup

The sealing between the microtube and the experimental loop was accomplished by Conax® packing glands consisting of a gland body and a sealant. The microtube was connected to the experimental loop from one side, whereas the other end was exposed to the atmosphere to ensure atmospheric conditions at the exit. To measure local temperatures, three thin Omega® thermocouple wires (~76 µm thick) was carefully installed to the microtube surface at desired locations using Omega® Bond. Thermocouples were located at x_{th1} = 1.82 cm, x_{th2} = 3.32 cm and x_{th3} = 4.82 cm over the heated length of 5.65cm. One additional Omega® thermocouple was installed upstream the inlet of the microtube to monitor the bulk temperatures at the inlet. Inlet pressures were measured via Omega® pressure transducers with a 0 to 100 psi gauge pressure range. Flow rate data was obtained together with the voltage, current, and wall/fluid temperatures, which were acquired through a LabView® interface with time and were transferred to a spreadsheet file for data reduction.

Experimental Procedure

The flow rate was fixed at the desired value by adjusting the pressure difference between the inlet and exit. It was made sure that temperature and pressure values obtained from LabView® interface did not significantly change with time so that experiments could be conducted after steady flow conditions were reached.

For the diabatic tests, the power was increased in 0.5 A increments. The current/voltage, inlet pressures and wall temperatures were acquired by acquisition rates of 100 data/s and averaged over time once steady state conditions were reached. This procedure was repeated for different flow rates.

To estimate the small heat losses, electrical power was applied to the test section before any fluid flow and experiment. The temperature difference between the ambient and the test section was recorded along with the corresponding power at steady state so that the power could be found as a function of surface temperature to calculate the heat loss ($\dot{Q}_{loss}$) associated with each experimental data point.

DATA REDUCTION

The data obtained from the voltage, current, flow rate, temperature and pressure measurements were used to obtain the friction factors, single-phase heat transfer coefficients and Nusselt numbers.

The friction factor, f is obtained from adiabatic tests and is given by:

$$f = \frac{2d_i \Delta p \rho_F}{LG^2} \qquad (1)$$

Using the above expression, f was evaluated for various mass velocities so that the change in f with Reynolds number was obtained. Reynolds number was expressed as:

$$\mathrm{Re} = Gd_i / \mu \qquad (2)$$

where G is the mass velocity and defined as:

$$G = \dot{m} / A_c \qquad (3)$$

For diabatic tests, the electrical input power and resistance were calculated using the measured voltage and current values. Assuming 1-D steady state heat conduction with uniform heat generation, the local inner surface temperature of the microchannel, $T_{w,i}$ is expressed in terms of the measured local outer surface temperature, $T_{w,o}$ as:

$$T_{w,i} = T_{w,o} + \frac{\dot{q}}{4k_w}\left(r_o^2 - r_i^2\right) - \frac{\dot{q}}{2k_w} r_o^2 \log\left(\frac{r_o}{r_i}\right) \qquad (4)$$

where $\dot{q}$ is the volumetric heat generation and expressed as a function of net power, inner channel radius, outer channel radius, and heated length as:

$$\dot{q} = \frac{\left(P - \dot{Q}_{loss}\right)}{\pi\left(r_o^2 - r_i^2\right)L_h} \qquad (5)$$

For single-phase flow, the single-phase heat transfer coefficient is obtained using the inner wall temperature and the net power:

$$h_{sp} = \frac{\left(P - \dot{Q}_{loss}\right)x_{th}}{A_s\left(\overline{T}_{w,i} - T_f\right)L_h} \qquad (6)$$

where inner surface area A_s is expressed as:

$$A_s = \pi d_i L_h \qquad (7)$$

Fluid temperatures are deduced from energy balance:

$$T_f = T_i + \frac{\left(P - \dot{Q}_{loss}\right)x_{th}}{\dot{m} c_p L_h} \qquad (8)$$

The Nusselt number is calculated using the average heat transfer coefficient obtained from Eq. (6) as:

$$Nu = \frac{h_{sp} d_i}{k_F} \qquad (9)$$

EES Software is used to reduce the experimental data to the desired above mentioned parameters in the current study.

Since fluid flows should be mostly considered as thermally developing flows under the conditions of the present study thermally developing flow correlations, which have been proposed by Shah and London [29] for laminar flows, are suitable to be used for the comparison with the experimental data. Thus, they could be used for predicting the experimental data (under laminar conditions):

$$Nu_{x,H1} = 0.517(f.Re)^{1/3}(x^*)^{-1/3} \quad (10)$$

$$Nu_{m,H1} = 0.775(f.Re)^{1/3}(x^*)^{-1/3} \quad (11)$$

where ;

$$x^* = \frac{x}{D_h RePr} \quad (12)$$

For turbulent flows, the following correlations, which have been proposed by Bhatti and Shah [30], have been used for thermally developing flows:

$$\frac{Nu_x}{Nu_\propto} = 1 + \frac{C_6}{10(\frac{x}{D_h})} \quad (13)$$

$$\frac{Nu_m}{Nu_\propto} = 1 + \frac{C_6}{(\frac{x}{D_h})} \quad (14)$$

where

$$C_6 = \frac{\left(\frac{x}{D_h}\right)^{0.1}}{Pr^{1/6}}(0.68 + \frac{3000}{Re^{0.81}}) \quad (15)$$

Nu_∞ in the above equations is the fully developed Nusselt number for thermally developing flows [30] and is expressed as:

$$Nu_\infty = 0{,}024(Re^{0.8})Pr^{0.4} \quad (16)$$

The uncertainties of the measured values are given in Table 1. They were provided by the manufacturer's specification sheet, whereas the uncertainties of friction factors and heat transfer coefficients were obtained using the propagation of uncertainty method developed by Kline and McClintock [31].

Uncertainity	Error
Flow Rate, Q (for each reading)	± 1.0 %
Voltage supplied by power source, V	± 0.1 %
Current supplied by power source, I	± 0.1 %
Temperature, T	± 0.1°C
Electrical power, P	± 0.15 %
Pressure drop, ΔP	± 0.25 %
Mass flux, G	± 2.7 %
Friction factor, f	± 7 %
Hydraulic diameter, d_h	± 2 μm
Heat transfer coefficient, h_{sp}	± 10.7 %
Nusselt number, Nu	± 11 %

Table 1 Uncertainties in experimental parameters

RESULTS AND DISCUSSIONS

Initially, adiabatic tests were carried out and satisfactorily compared to the existing conventional friction factor correlation recommended for laminar flows in tubes (f=64/Re). As shown in Fig. 2, experimental data could be predicted fairly well by the existing correlation for laminar flow conditions with a MAE of 21%. This result is in agreement with the previous comparison studies on friction factors [4, 6, 20, 21], which also reported that friction factors in microchannels in fully developed flow could be predicted by the existing theory developed for conventional channels. Moreover, this fair prediction also implies that hydrodynamically developed flow conditions are present in the current study. The hydrodynamic developing length for Re=1087 is 1.5cm, which is significantly lower than the entire channel length of 14.88 cm. Thus, hydrodynamic fully developed flow conditions are not expected in this study.

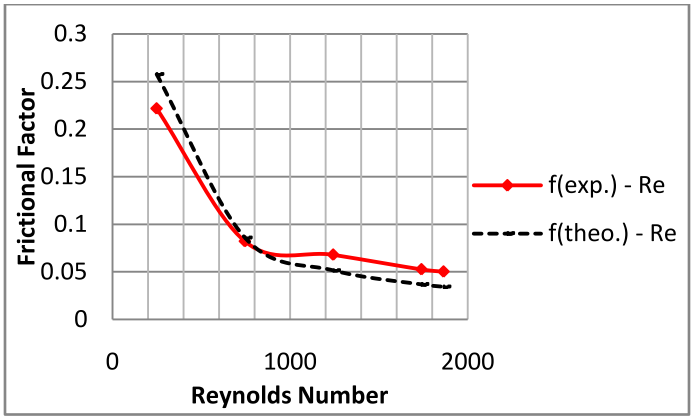

Figure 2 Friction Factors-Reynolds Number profile

In addition to these findings, adiabatic tests have been also carried out for the same microchannel configuration to observe laminar-turbulent transition. The transition from laminar flow to turbulent flow for the same configuration is detected with the shift in the trend of f vs Re curve (Fig. 3). It can be seen that the transition of Reynolds number occurs between 2500-3000 due to the change in the trend, which could not be characterized as an early transition. This transition could be also regarded as a sudden transition [4]. Lorenzini et al.[4] indicated that sudden laminar to turbulent transition seems to become the prevailing mode when the critical Reynolds number is greater than the 2300 regardless of the surface of the microtubes (i.e. either smooth or rough). As a result, laminar to turbulent transition in this study could be also regarded as a sudden transition.

For the turbulent portion of the experimental data, Colebrook correlation was used and compared to experimental data. A relative roughness was taken as 0.004 in the light of measured peak to peak roughness and microtube dimensions.

Accordingly, the MAE in friction factor is calculated as 19.3%, which suggests that friction factor correlations for turbulent flows could also fairly predict turbulent flow data in micro scale. These results are in good agreement with the existing literature on micro scale [4, 18].

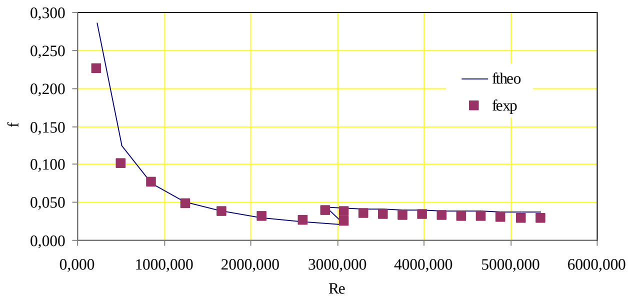

Figure 3 Friction Factors-Reynolds Number profile

Heat Transfer Results

In Figs. 4-6, local single phase heat transfer coefficients were presented for each thermocouple location at different mass fluxes. As seen from these figures, single phase heat transfer increases as mass flux increases. In addition, we can observe that the increase in mass flux results in lower channel surface temperatures at constant heat fluxes. The increasing trend in local heat transfer coefficients with mass flux is due to developing flow conditions and also provides high motivation for working at high mass fluxes since high heat fluxes so that high heat transfer coefficients could be reached even in single phase flow (>200 W/cm^2) as seen in Figs. 4-6. These displayed heat flux values are much greater than the literature studies [20] due to the high mass fluxes and thermally developing flow conditions.

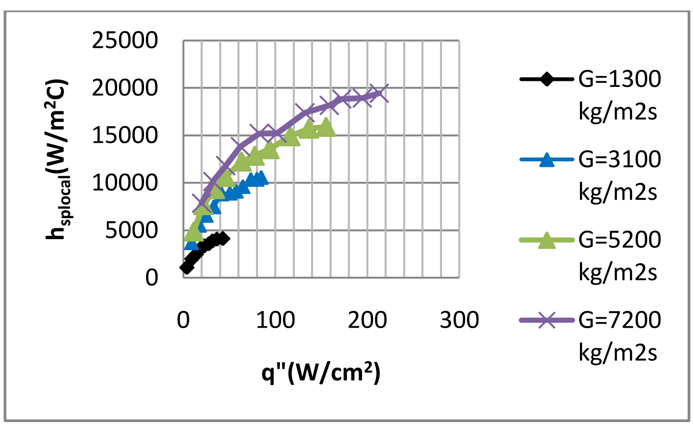

Figure 4 Local single phase heat transfer coefficients – heat flux profile for thermocouple 1

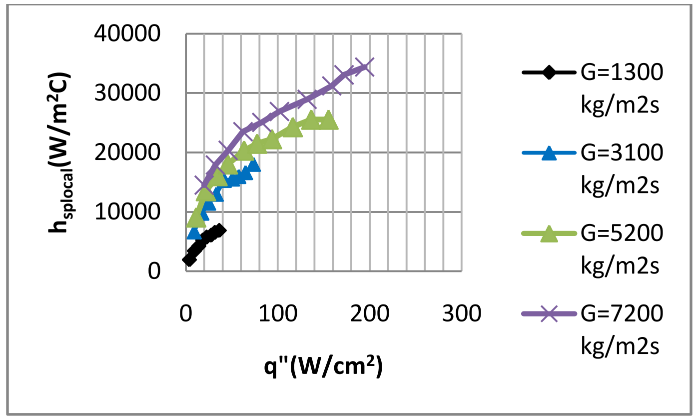

Figure 5 Local single phase heat transfer coefficients – heat flux profile for thermocouple 2

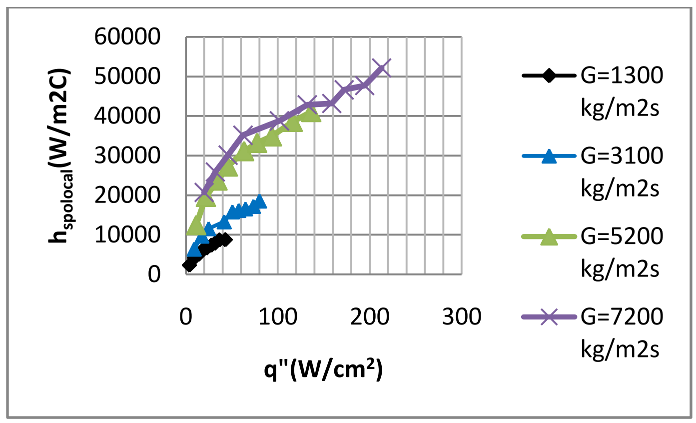

Figure 6 Local single phase heat transfer coefficients – heat flux profile for thermocouple 3

The comparison between theoretical and experimental Nusselt numbers is demonstrated in Figs. 7-9 for each thermocouple location. $Nu_{x,H1}$ is the theoretical thermally developing Nusselt number depending on the location x, while Nu is the corresponding experimental Nusselt number. For laminar flow conditions, Eq. 10 was used for calculating $Nu_{x,H1}$, while under turbulent conditions Eq. 13 was used for calculating $Nu_{x,H1}$. As seen from these figures almost every data point could be predicted within ± 50 % by the existing correlations. The resulting total MAE is 24%. These results show that experimental Nusselt numbers could be reasonably predicted by theoretical Nusselt numbers for developing flow conditions. This also strengthens the claim in the literature [29, 30] that conventional correlations could be applicable to single-phase flows in micro scale. However, they could not follow the trend very well. In addition, the success of thermally developing flow correlations also emphasize on developing effects on heat transfer. The thermally developing lengths for G=1300, 3100, 5200 and 7200 are 3.5cm, 7.1cm, 11.22cm and 15.74cm respectively, which are greater than the heated length of the microtube. Thus, developing effects are prevalent along the entire heated length leading to high heat transfer coefficients and Nusselt numbers when compared to thermally fully developed flows.

For thermocouple locations 1 and 2 the experimental results are closer to the theory (MAE=19.2, 20.8, respectively) compared to thermocouple location 3 (MAE=23.6). It can be clearly seen that while Re increases experimental data results better agree with the theoretical results for thermocouple locations 1 and 2. This trend is present because thermocouples 1 and 2 are located closer to the micro tube inlet, where developing effects are more dominant. Figs. 7-9 show similar trend with literature studies [5, 19]. Moreover, increasing with mass fluxes experimental results approach to the theoretical predictions. Because, while mass flux increase thermally developing lengths increase too.

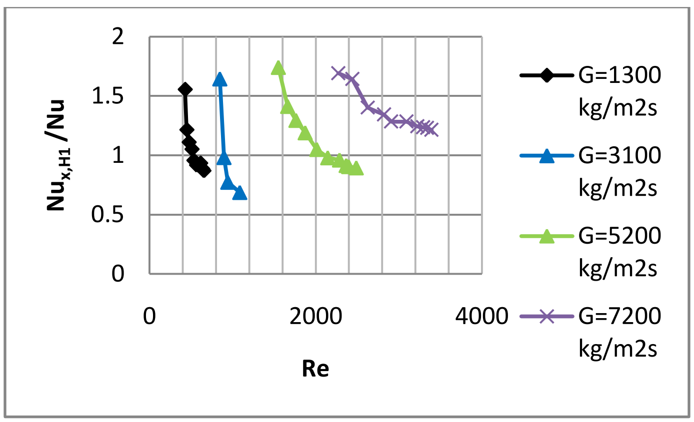

Figure 7 Ratio of theoretical Nusselt number to experimental Nusselt number for thermocouple 1

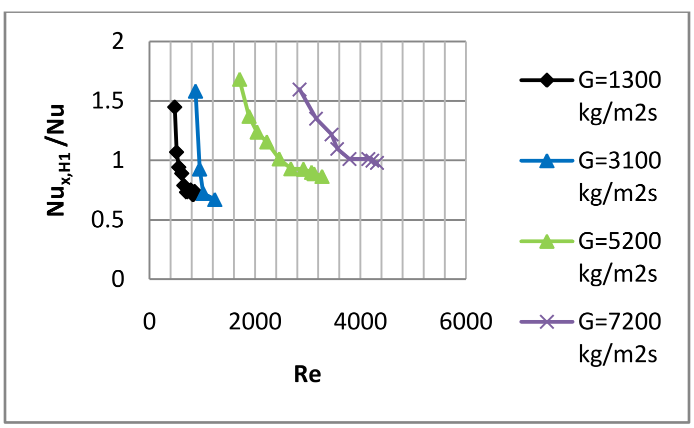

Figure 8 Ratio of theoretical Nusselt number to experimental Nusselt number for thermocouple 2

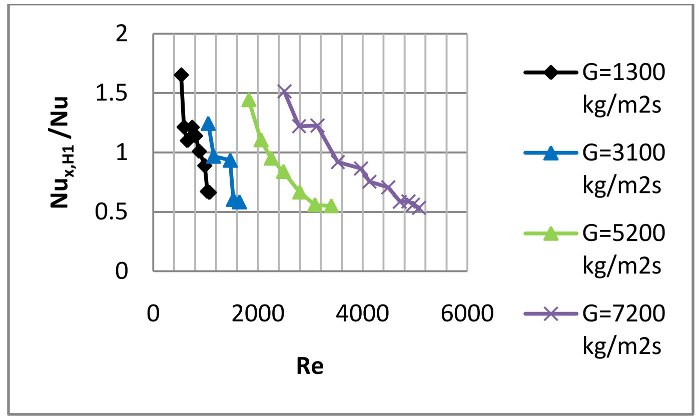

Figure 9 Ratio of theoretical Nusselt number to experimental Nusselt number for thermocouple 3

CONCLUSION

Experimental tests were carried out in a micro tube of ~254 µm inner diameter at mass velocities *G*=1300-7200 kg/m^{2}s under thermally developing flow conditions. Higher single phase heat transfer coefficients were obtained with high mass fluxes, which is motivating to operate at high mass fluxes and under developing flow conditions. Theoretical friction factors and Nusselt numbers were compared to the experimental findings. A reasonable agreement was found between experimental results and theoretical predictions recommended for heat transfer in thermally developing flows. Moreover, the transition to turbulent flow and friction factors for both laminar and turbulent conditions were in agreement with conventional correlations and existing theory. As a future work, it is aimed that operating at higher mass fluxes and the using microchannels of different inner diameters.

ACKNOWLEDGMENTS

This work was supported by TUBITAK (The Scientific and Technological Research Council of Turkey) Support Program for Scientific and Technological Research Projects Grant, 107M514. Graduate student support provided by the Faculty of Engineering and Natural Sciences of Sabancı University is greatly appreciated.

REFERENCES

[1] Kandlikar, S.G., 2006, “Single-phase liquid flow in minichannels and microchannels”, Heat Transfer and Fluid Flow in Minichannels and Microchannels, pp. 87-136.

[2] Owhaib, W. and Palm, B., 2004, “Experimental investigation of single-phase convective heat transfer in circular

microchannels", Experimental Thermal and Fluid Science, 28(2-3), pp. 105-110.

[3] Hrnjak, P. and Tu, X., "Single phase pressure drop in microchannels", International Journal of Heat and Fluid Flow, 28(1), pp. 2-14.

[4] Lorenzini, M., Morini G. L., and Salvigni, S., 2010, "Laminar, transitional and turbulent friciton factors for gas flows in smooth and rough microtubes", International Journal of Thermal Sciences, 49(2), pp. 248-255.

[5] Celata, G.P., Cumo M., McPhail, S.J., and Zummo G., 2007, "Single-phase laminar and turbulent heat transfer in smooth and rough microtubes", Journal of microfluid and nanofluid, 3, pp. 697-707.

[6] Morini, G.L., 2004, "Single-phase convective heat transfer in microchannels: a review of experimental results", International Journal of Thermal Sciences, 43(7), pp. 631-651.

[7] Hetsroni, G., Mosyak, A., Pogrebnyak, E., and Yarin, L.P., 2005, "Fluid flow in micro-channels", International Journal of Heat and Mass Transfer, 48, pp. 1982-1998.

[8] Lee, P. and Garimella S.V., 2006, "Thermally developing flow and heat transfer in rectangular microchannels of different aspect ratio", International Journal of Heat and Mass Transfer, 49, pp. 3060-3067.

[9] Morini, G.L., 2004, "Laminar-to-Turbulent flow transition in microchannels", Microscale Thermophys. Eng., 8, pp. 15-30.

[10] Obot, N.T., 2002, "Toward a better understanding of friction and heat/mass transfer in microchannels-a literature review, Microscale Thermophys. Eng., 6, pp. 155-173.

[11] Choi, S.B., Barron, R.F., and Warrington, R.O, 1991, "Fluid flow and heat transfer in microtubes in: Micromechanical Sensors, Actuators and Systems, ASME DSC, Atlanta, GA, pp. 123-134.

[12] Ghiaasiaan, S.M. and Laker, T.S., 2001, "Turbulent forced convection in microtubes", International Journal of Heat and Mass Transfer, 44(14), pp. 2777-2782.

[13] Hao, P-F., Zhang, X-W., Yao, Z-H., and He, F., 2007, "Transitional and turbulent flow in a circular microtube", Experimental Thermal and Fluid Science, 32(2), pp. 423-431.

[14] Adams, T.M, Dowling, M.F., Abdel-Khalik, S.I., and Jeter, S.M., 1999, "Applicability of traditional turbulent single-phase forced convection correlations to non-circular microchannels", International Journal of Heat and Mass Transfer, 42(23), pp. 4411-4415.

[15] Yang, W-H., Zhang, J-Z. and Cheng, H.E., 2005, "The study of flow characteristics of curved microchannel", Applied Thermal Engineering, 25(13), pp. 1894-1907.

[16] Shen, S., Xu, J.L., Zhou, J.J., and Chen, Y., 2006, "Flow and heat transfer in microchannels with rough wall surfaces", Energy Conversion and Management, 47(11-12), pp. 1311-1325.

[17] Mishan, Y., Mosyak, A., Pogrebnyak, E., and Hetsroni, G., 2007, "Effect of developing flow and thermal regime on momentum and heat transfer in micro-scale heat sink", International Journal of Heat and Mass Transfer, 50(15-16), pp. 3100-3114.

[18] Steinke, M.E., and Kandlikar, S.G., 2006, "Single-phase liquid friction factors in microchannels", International Journal of Thermal Sciences, 45(11), pp. 1073-1083.

[19] Baviere, R., Favre-Marinet, M., and Le Person, S., 2006, "Bias effect on heat transfer measurements in microchannel flows", International Journal of Heat and Mass Transfer, 49(19-20), pp. 3325-3337.

[20] Caney, N., Marty, P., and Bigot, J., 2007, "Friction losses and heat transfer of single-phase flow in a mini-channel", Applied Thermal Engineering, 27, pp. 1715-1721.

[21] Rands, C., Webb, B.W., and Maynes, D., 2006, "Characterization of transition to turbulence in microchannels", International Journal of Heat and Mass Transfer, 49(17-18), pp. 2924-2930.

[22] Khlebtsov, G.N. and Dykman, L.A., 2010, "Optical properties and biomedical applications of plasmonic nanoparticles", Journal of Quantitative Spectroscopy and Radiative Transfer, 111(1), pp. 1-35.

[23] Baffou, G., Quidant, R., and Abajo, F.J.G., 2010, "Nanoscale Control of Optical Heating in Complex Plasmonic Systems", ACSNANO, *In Press*.

[24] DiMatteo, R.S., Greiff, P., Finberg, S.L., Young-Waithe, K., Choy, H.K.H., Masaki, M.M., and Fonstad, C.G., 2001, "Enhanced photogeneration of carriers in a semiconductor via coupling across a nonisothermal nanoscale vacuum gap", Appl. Phys. Lett., 79, pp. 1894.

[25] Francoeur, M., Menguc, M.P., and R. Vaillon, 2008, "Near-field radiative heat transfer enhancement via surface phonon-polaritons coupling in thin films," *Appl. Phys. Lett.*, 93, 043109.

[26] Fu, C.J. and Tan, W.C., 2009, "Near-field radiative heat transfer between two plane surfaces with one having a

dielectric coating”, Journal of Quantitative Spectroscopy and Radiative Transfer, 110(12), pp. 1027-1036.

[27] Sendur, K., Peng, C., and Challener, W., 2005, “Near field radiation from a ridge waveguide transducer in the vicinity of a solid immersion lens”, Phys. Rev. Lett., 94, pp. 043901.

[28] Francoeur, M., Menguc, M.P., and R. Vaillon, 2010, “Near-field radiative heat exchanges between two thin films supporting surface phonon-polaritons," *J. Appl. Phys.* (in press).

[29] Shah, R.K. and Sekulic, D.P., 2003, Fundamentals of Heat Exchanger Design, John Wiley&Sons, pp. 502-505

[30] Shah, R.K. and Sekulic, D.P., 2003, Fundamentals of Heat Exchanger Design, John Wiley&Sons, pp. 505-506

[31] Kline, S. and McClintock, F.A., 1953, “Describing Uncertainties in Single-Sample Experiments,” Mech. Eng. (Am. Soc. Mech. Eng.), 75(1), pp. 3-8.

[32] Munson, B.R., Young, D.F., and Okiishi, T.H., Fundamentals of Fluid Mechanics, John Wiley&Sons, pp. 431-435